Antiphase domain and magnetic interactions in partially ordered Ni_3Mn

A. Paciaroni, C. Petrillo, and F. Sacchetti
Dipartimento di Fisica, Università di Perugia, Via A. Pascoli, I-06100 Perugia, Italy
and Istituto Nazionale per la Fisica della Materia, Unitá di Perugia, Perugia, Italy
(Received 21 February 1995)

An experimental study of the antiphase domains originating from both nuclear and magnetic ordering processes in the partially ordered compound $Ni_{78}Mn_{22}$ was carried out by means of polarized neutron diffraction. The analysis of the data collected at several temperatures in the range 40–573 K allowed us to deduce the size distribution of magnetic and nuclear antiphase boundaries and to further investigate the role of second-nearest-neighbor interactions on the magnetic properties of this system.

I. INTRODUCTION

The magnetic behavior of fcc $3d$ Mn-based alloys, among which Co_xMn_{1-x} and Ni_xMn_{1-x} are examples of the variety of magnetic structures arising from composition and temperature variations,[1,2] is the subject of several investigations. Recently, Cable and Tsunoda[3] examined in detail the disordered phases of both Co_xMn_{1-x} and Ni_xMn_{1-x} alloys in the concentration region intermediate between ferromagnetic and antiferromagnetic long-range order. The magnetic properties of the partially ordered phase that can be stabilized in the intermetallic compound $Ni_{78}Mn_{22}$ were investigated in Refs. 4–6 by means of polarized neutron diffraction. In particular, two different states of long-range order and the behavior of the local magnetic moments versus temperature were studied. The main findings of these measurements were that Mn atoms in this compound have a magnetic moment of about $4\mu_B$ with fluctuating sign (spin reversal) and that the magnetic ordering of chemically ordered $Ni_{78}Mn_{22}$ is dominated by first-nearest-neighbor interactions. The complex features exhibited by this system when the state of order is changed, are connected to the presence of competing ferromagnetic (Ni-Ni and Ni-Mn) and antiferromagnetic (Mn-Mn) first-nearest-neighbor interactions. As a consequence, the behavior of the Mn magnetic moment is directly related to the configuration of the first shell. The possible influence of the second-nearest-neighbor shell and beyond seems to be confined to secondary contributions hardly detectable by the neutron-diffraction experiments of Refs. 4–6.

In order to ascertain the possible role played by interactions beyond the first-nearest neighbors in defining the magnetic behavior of $Ni_{78}Mn_{22}$ and to add further information on the first-nearest-neighbor interactions, we performed an experimental study of the antiphase domains originating from both nuclear and magnetic ordering processes. The relevance of studying the antiphase domain boundary in ordered crystals with $L1_2$ (Cu_3Au) structure, relies on the property that atoms at the boundary have the *same* first-nearest neighbors as those inside the domain.[7] Therefore all the effects due to the presence of antiphase domains are related to second-nearest-neighbor interactions. Strictly speaking this behavior refers to fully ordered stoichiometric alloys, since the environment of an atom not occupying its regular site is different when it is inside a domain or at an antiphase boundary.

The appearance of the antiphase domains in $Ni_{78}Mn_{22}$ was investigated carrying out a polarized neutron-diffraction experiment properly designed to determine the distribution of the antiphase boundaries along a cube edge direction. Measurements were performed at various temperatures in order to study the temperature dependence of the antiphase domains. Moreover phenomena arising from purely magnetic ordering could be identified allowing us to analyze the magnetic behavior at the boundary region.

II. EXPERIMENT AND DATA ANALYSIS

As described in Ref. 7, the presence of randomly distributed antiphase domains in $L1_2$ ordered systems is revealed by a *pronounced broadening* of the superlattice Bragg reflections, the shape of the fundamental ones being not appreciably affected by this. The detailed description of this effect and the calculation of the expected Bragg reflection intensities in the case of a system interacting through purely first-nearest-neighbor interactions are carried out in Ref. 7. Using symmetry arguments, the antiphase boundaries in $L1_2$ structures should lie along the cube edge directions, even though they are not necessarily equally distributed along different directions. In the present experiment only one crystallographic direction was investigated to adopt the simplest experimental geometry.

The neutron-diffraction experiment was performed using the polarized-neutron diffractometer installed at the 1-MW Training, Research and Isotope Production Reactor of Centro Ricerche Energia, Casaccia (Rome). The polarized and monochromatic neutron beam was produced by means of a $Co_{92}Fe_8$ monochromator, the neutron spin was reversed at 3 Hz frequency. The scattered beam was detected in the horizontal plane and the diffracted intensity was separately collected for the two spin states of the incoming neutron. The sample was magnetized at saturation by a vertical magnetic field of

0.7 T. It was the same as used in Refs. 4–6, slab shaped, $1\times1.8\times0.07$ cm^3 dimensions with the extended face parallel to the (100) plane. The chemical and magnetic state of the present sample as a function of both temperature and state of order is described in Refs. 4–6. The value of the long-range order parameter S, defined as the ratio between the measured scattering amplitude of a superlattice reflection and the scattering amplitude expected for the ideally ordered stoichiometric sample, was found to be 0.553(4). Actually, the long-range order parameter was deduced by measuring the integrated intensity ratio of superlattice to fundamental reflections. By such a procedure, the absolute measurement of the superlattice intensity is avoided and the result is independent of whether or not antiphase domains exist in the sample. Although antiphase boundaries broaden the superlattice reflection, they do not affect the integrated intensity of the peak.[7]

In the present experiment, the rocking curve of the (100) reflection was measured for both the spin states of the incoming neutron and as a function of the temperature in the temperature range from 40 to 573 K. As a reference, the rocking curve of the fundamental (200) reflection was measured at room temperature. The instrumental resolution was evaluated by measuring the rocking curve of the (200) reflection of an almost perfect KBr single crystal. The d spacing for such a reflection is very close to that of the (100) superlattice reflection in $Ni_{78}Mn_{22}$ and hence both occur at approximately the same scattering angle. In Fig. 1 an example of (100) rocking curves for both *up* and *down* neutron spin is shown together with the (200) rocking curves of $Ni_{78}Mn_{22}$ and KBr. The rocking curve of the (100) reflection is much broader than both the fundamental (200) and the resolution of the diffractometer as measured by the KBr rocking curve, thus confirming the presence of antiphase boundaries within the sample. Additional measurements on the $Ni_{78}Mn_{22}$ sample were carried out by performing a series of $(\omega, 2\vartheta)$ scans around the (100) reflection. Since, as discussed in Ref. 7, the intensity distribution at a superlattice point has approximately the shape of a thin disk properly oriented, the (100) rocking curve and the $(\omega,2\vartheta)$ scan will cross the disk along different directions. In Fig. 2(a) the $(\omega,2\vartheta)$ scan parallel to the [100] direction is compared to the (100) rocking curve that corresponds to a scan roughly orthogonal to the [100] direction. As expected, the $(\omega,2\vartheta)$ curve is much more narrow than the rocking curve, thus indicating that the plane of the disk is perpendicular to the [100] direction, as discussed in Ref. 7. In Fig. 2(b) a three-dimensional view of the intensity collected along both the scans is presented.

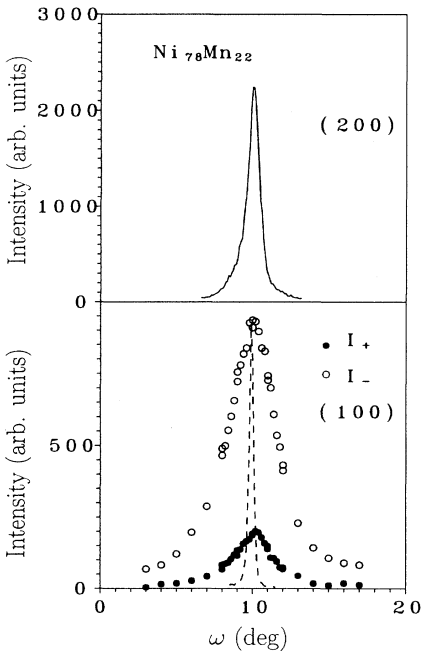

FIG. 1. Upper panel: rocking curve of the (200) reflection in $Ni_{78}Mn_{22}$. Lower panel: rocking curves of the (100) reflection in $Ni_{78}Mn_{22}$ for *up* (dots) and *down* (circles) spin states of the incoming neutron. The dashed line is the (200) rocking curve of a nearly perfect KBr single crystal whose peak intensity has been normalized for comparison purposes. All the data refer to room-temperature measurements.

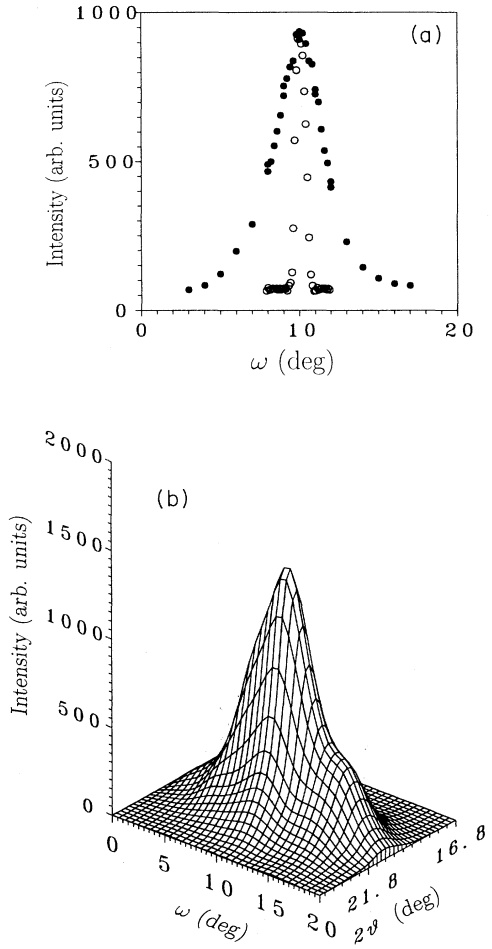

FIG. 2. (a) $(\omega,2\vartheta)$ scan along [100] direction (circles) in comparison with the (100) rocking curve (dots) in $Ni_{78}Mn_{22}$. Room-temperature measurements. (b) Intensity versus ω and 2ϑ as measured by $(\omega,2\vartheta)$ and rocking scans.

From the present data, the size distribution of the domains can be obtained starting from the general expression of the nuclear-scattering cross section in an AB_3 compound with $L1_2$ ordered structure, that is,

$$\left[\frac{d\sigma}{d\Omega}\right]_N = |F_N^{(L)}|^2 \sum_{ll'} p_l p_{l'} e^{i\mathbf{Q}\cdot(\mathbf{R}_l-\mathbf{R}_{l'})}, \quad (1)$$

where $F_N^{(L)}$ is the nuclear structure factor of a superlattice reflection and $F_N^{(L)}=b_A-b_B, b_A$ and b_B being the nuclear scattering amplitudes of the A and B sites. For the ideally ordered stoichiometric system, A sites (corners) are occupied by Mn and B sites (faces) by Ni. The parameter p_l identifies the lth site as belonging to one of the two antiphase domains and it is equal to $(+1)$ for one kind of ordering and to (-1) for the opposite one. The sum runs over all the atomic sites in the sample. Following the procedure described in Ref. 7 and through Eq. (1), the nuclear-scattering intensity I_N collected along the rocking curve can be written as

$$I_N \propto |F_N^{(L)}|^2 \frac{R_N}{a_0} \frac{\Gamma_N}{Q^2+\Gamma_N^2} = F_N^2(Q), \quad (2)$$

where R_N is the *average* distance between two antiphase boundaries and $\Gamma_N=2R_N/a_0, a_0$ being the lattice parameter. In a system where the magnetic moments are completely localized at the atomic sites and their values depend on the atomic species only, the magnetic contribution to the scattering at a superlattice line behaves exactly as the nuclear contribution. However, for more complex magnetic structures, the shape of the magnetic contribution to the scattering along the rocking curve can be different from the nuclear one. By means of a polarized neutron beam, as for the present experiment, it is rather easy to distinguish between magnetic and nuclear contributions, since the intensity diffracted along the rocking curve depends on the spin state of the incoming neutrons. For an incoming beam polarization perpendicular to the scattering plane and parallel to the magnetization direction of the ferromagnetic sample, the intensities for parallel (I_+) and antiparallel (I_-) spin states of the incoming neutron are given by

$$I_\pm = F_N^2(Q) + F_M^2(Q) \pm 2P_{(\pm)} F_N(Q) F_M(Q). \quad (3)$$

$P_{(\pm)}$ is the neutron polarization in the two spin states and $F_N(Q)$ is the shape function describing the chemical antiphase domain distributions defined in Eq. (2). The shape function $F_M(Q)$, that embodies the distribution of the magnetic antiphase domains, is still defined by Eq. (2) using for the relevant quantities their magnetic counterparts, that is

$$F_M^2(Q) = |F_M^{(L)}|^2 \frac{R_M}{a_0} \frac{\Gamma_M}{Q^2+\Gamma_M^2} \quad (4)$$

with $F_M^{(L)}=p_A(Q)-p_B(Q)p_A(Q)$ and $p_B(Q)$ being the magnetic scattering amplitudes of the A and B sites. Through Eq. (3), with I_+ and I_- measured quantities, it is possible to separately deduce the shape functions for nuclear and magnetic scattering. In Fig. 3 the magnetic and nuclear contributions along the (100) rocking curve, as measured at room temperature, are shown. The comparison enhances the different widths of the two curves. This is an immediate evidence that the distribution of the antiphase boundaries is not the same for chemical and magnetic ordering.

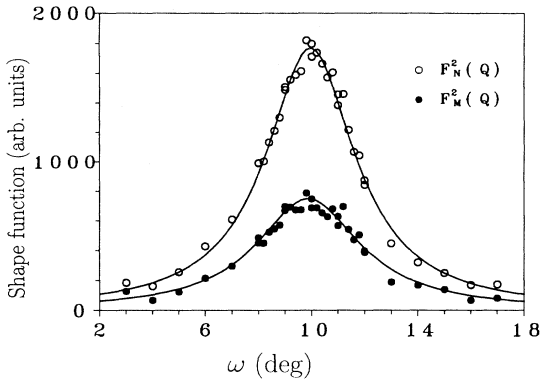

FIG. 3. Magnetic (dots) and nuclear (circles) shape functions of (100) reflection at room temperature. The full curves are the Lorentzian functions fitted to the data according to the model described in the text.

Further information about the magnetic and nuclear shape functions was gained by the measurements of $I_\pm$ versus temperature in the range from 40 to 573 K. For a closer comparison among the different sets of data, we fitted the $F_N^2(Q)$ and $F_M^2(Q)$ functions, deduced from the experimental data at the various temperatures, using Lorentzian functions as given in Eqs. (2) and (4). This model fits well the experimental data over the whole temperature range and a typical result is shown in Fig. 3. The nuclear $(2\Gamma_N)$ and magnetic $(2\Gamma_M)$ widths thus obtained are reported in Fig. 4 as a function of the temperature. The nuclear width was found to be independent of the temperature, within the statistical errors, as expected considering that there is no evolution of the chemical state of order over the present temperature range. The state of order can indeed be changed only approaching

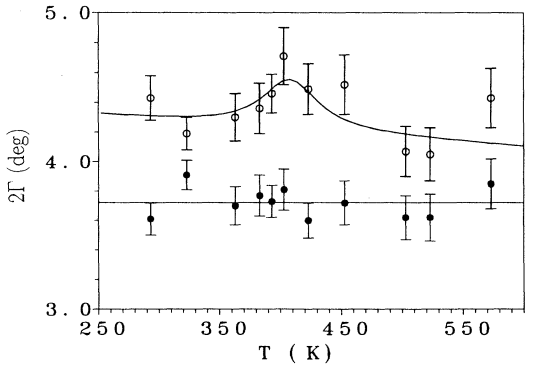

FIG. 4. Full width at half maximum of magnetic (dots) and nuclear (circles) shape functions as a function of the temperature.

higher temperatures and for a very long annealing time.[5] In other words, the activation energy necessary to create an antiphase boundary is much higher than the thermal energy $k_B T$, in the temperature range presently explored. From the whole of the experimental data collected at the various temperatures, the average length of the chemical antiphase domains was deduced. We obtained a value $R_N = 34.8 \pm 0.4$ Å, which corresponds to about ten unit cells. The meaning of this result is within the picture of an *almost random distribution* of antiphase boundaries with *average* distance equal to R_N.

For what concerns the magnetic contribution, the distribution of the magnetic antiphase boundaries was found to be quite different from that related to the chemical ordering. In particular the value $R_M = 30.4 \pm 0.4$ Å, which corresponds to slightly less than nine unit cells, was found. The difference between the results for chemical and magnetic antiphase domains, $R_N - R_M = 4.4 \pm 0.6$ Å, amounts practically to one unit cell. Finally, the data shown in Fig. 4 suggest a possible, although very small, temperature dependence of the magnetic width. However, much higher statistical accuracy is necessary to confirm this trend.

The present results are a clear evidence that the magnetic ordering in the $Ni_{78}Mn_{22}$ sample does not closely follow the chemical ordering, that is the magnetic moment depends on the local environment of each atom. Since the difference between R_N and R_M corresponds to one unit cell, there is a reasonable indication that the effect of the local environment on the magnetic moments is confined to first-nearest neighbors. We believe that the observed behavior is due to those Mn atoms located at the wrong sites on the planes where an antiphase boundary occurs. For these sites the local environment is different from that inside the antiphase domain and the magnetic moment of these atoms is consequently changed from that occurring in the bulk of the domains. Such a behavior is in agreement with the general trend observed for the Mn magnetic moment versus the state of order[5] and it gives further strength to the hypothesis that the Mn magnetic moment changes accordingly to the local distribution of first-nearest neighbors.

[1]A. Z. Menshikov, G. A. Takzei, Yu. A. Dorofeev, V. A. Kazantsev, A. K. Kostyshin, and I. I. Sych, Sov. Phys. JETP **62**, 734 (1985).

[2]W. Abdul-Razzaq and J. S. Kouvel, Phys. Rev. B **35**, 1764 (1987).

[3]J. W. Cable and Y. Tsunoda, Phys. Rev. B **50**, 9200 (1994), and references therein.

[4]C. Petrillo, F. Sacchetti, and M. Scafi, Phys. Rev. B **44**, 9418 (1991).

[5]G. Mazzone, C. Petrillo, F. Sacchetti, and M. Scafi, Phys. Rev. B **46**, 11 665 (1992).

[6]G. Mazzone, C. Petrillo, and F. Sacchetti, Phys. Rev. B **49**, 4307 (1994).

[7]B. E. Warren, *X-Ray Diffraction* (Addison-Wesley, New York, 1969), Chap. 12.